The Search for *Helical* Intergalactic Magnetic Fields

Tanmay Vachaspati

Cosmology Initiative

Arizona State University

Based on:

H. Tashiro, W. Chen, F. Ferrer & T. Vachaspati, MNRAS Lett. 445(1), L41 (2014);
H. Tashiro & T. Vachaspati, MNRAS 448, 299 (2015) ;
W. Chen, B. Chowdhury, F. Ferrer, H. Tashiro & T. Vachaspati, MNRAS 450, 3371 (2015).
A. Long & T. Vachaspati, MNRAS (2015).

Why helical?

Protected: Helicity is conserved in ideal MHD.

Inverse cascade: Evolution from small to large length scales.

Predicted in matter-genesis scenarios: via baryon # violation.

Enhances detectability: via parity odd signature.

Baryon number violation produces helical magnetic fields.

$$\boxed{\mathcal{H}(t) = \int d^3x \ \mathbf{A} \cdot \mathbf{B}}$$

Baryon number violation in standard model proceeds via a “sphaleron”.

- sphaleron = twisted monopole-antimonopole

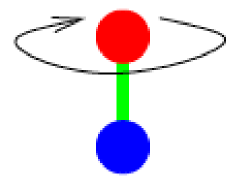

Taubes;
Manton;
Manton&Klinkhamer;
TV & Field;
Hindmarsh & James.

- sphaleron decay produces helical **B** (numerical and analytical)

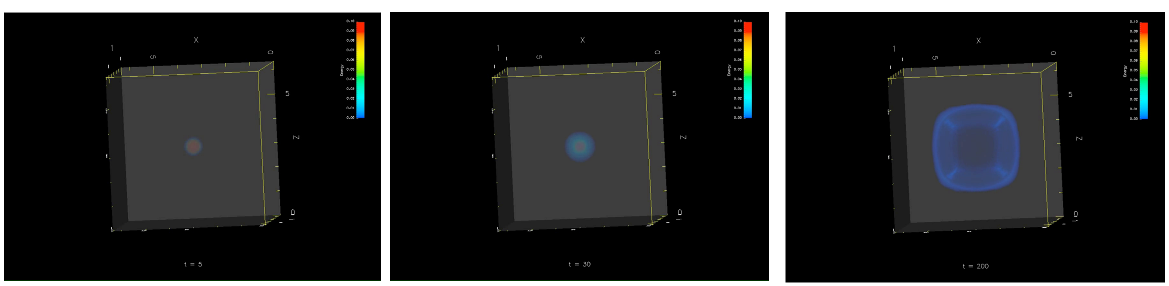

Copi, Ferrer, TV & Achucarro, 2008
Diaz-Gil, Garcia-Bellido, Perez & Gonzalez-Arroyo, 2008
Chen, Dent & TV, 2010

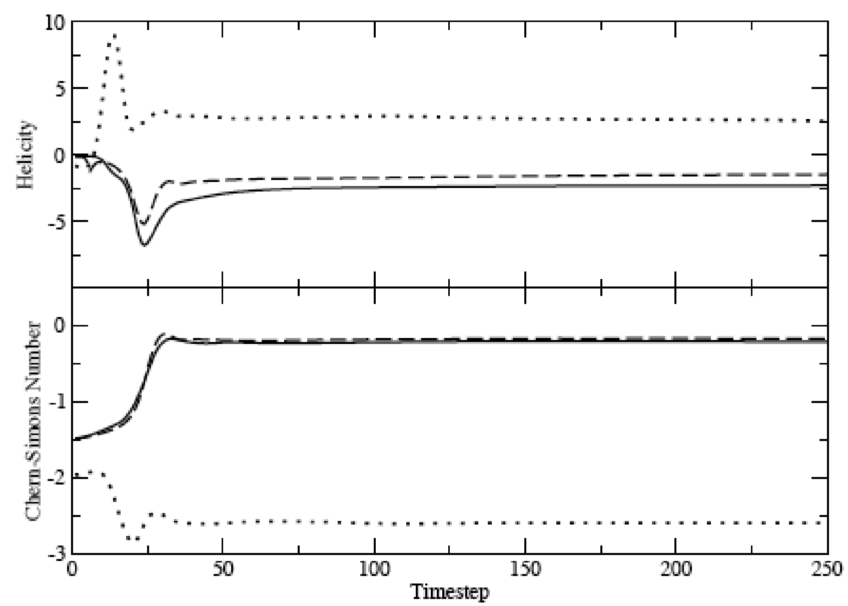

Cosmological magnetic helicity

$$\text{Every } \Delta B \implies \Delta\mathcal{H}$$

J. Cornwall
TV

$$\implies \quad \boxed{h \approx -\#\frac{n_b}{\alpha}}$$

Statistical Description:

$$\langle B_i(\mathbf{x}+\mathbf{r})B_j(\mathbf{x})\rangle = M_N(r)\left[\delta_{ij} - \frac{r_i r_j}{r^2}\right] + M_L(r)\frac{r_i r_j}{r^2} + M_H(r)\epsilon_{ijl}r^l$$

What is a good strategy to detect & measure magnetic helicity?

i.e. not just B but the twisting of B.

Kahniashvili & Vachaspati, 2006 (cosmic rays)
Tashiro & Vachaspati, 2013 & 2015 (gamma rays)

Cascade halos from TeV blazars

Gould & Schreder, 1967; Coppi & Aharonian, 1998; ..... Neronov & Semikoz, 2009

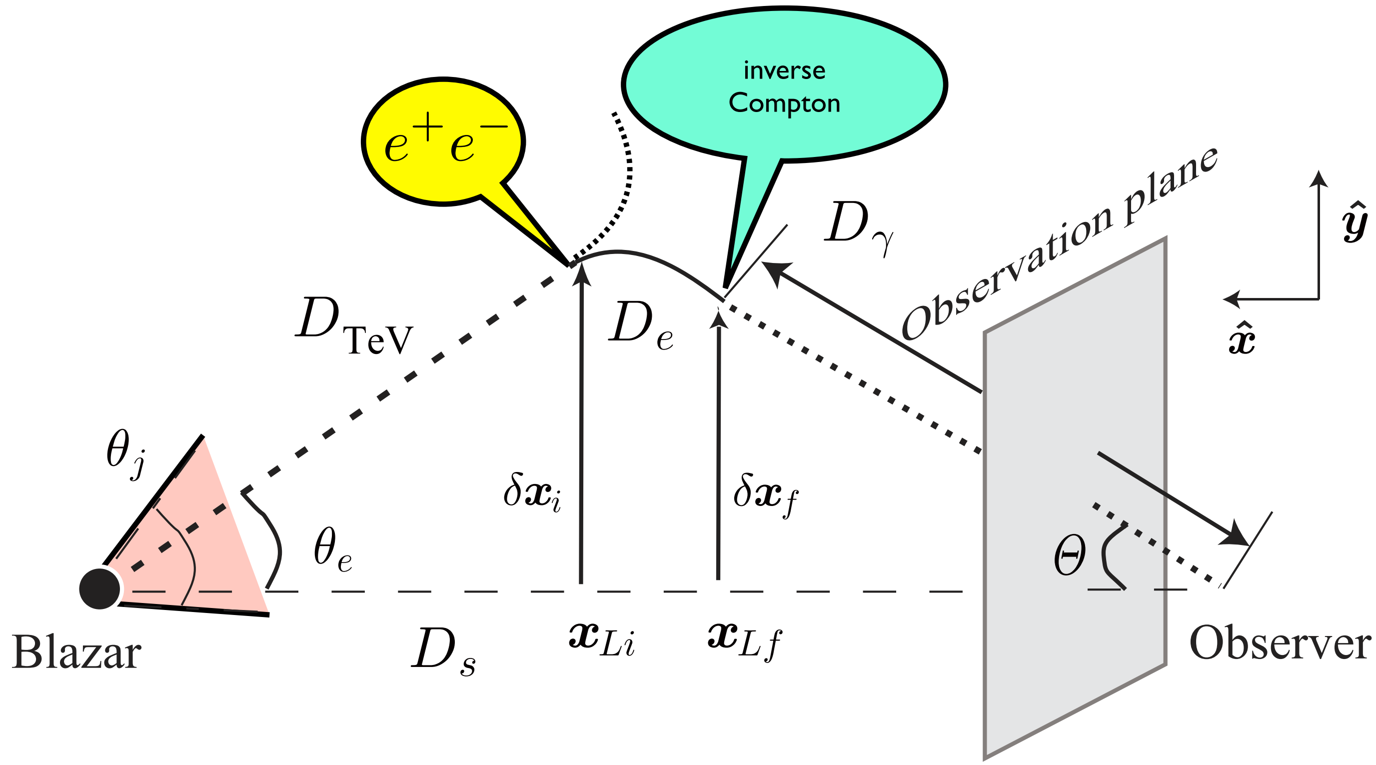

$$D_{\rm TeV} \sim 100 \text{ Mpc}, \quad D_e \sim 30 \text{ kpc}, \quad D_\gamma \sim D_s \sim 1 \text{ Gpc}$$

A Lower Bound? B-Detection?

Neronov & Vovk, 2010; Ando & Kusenko, 2010; Essey, Ando & Kusenko, 2011; Chen, Buckley & Ferrer, 2015.

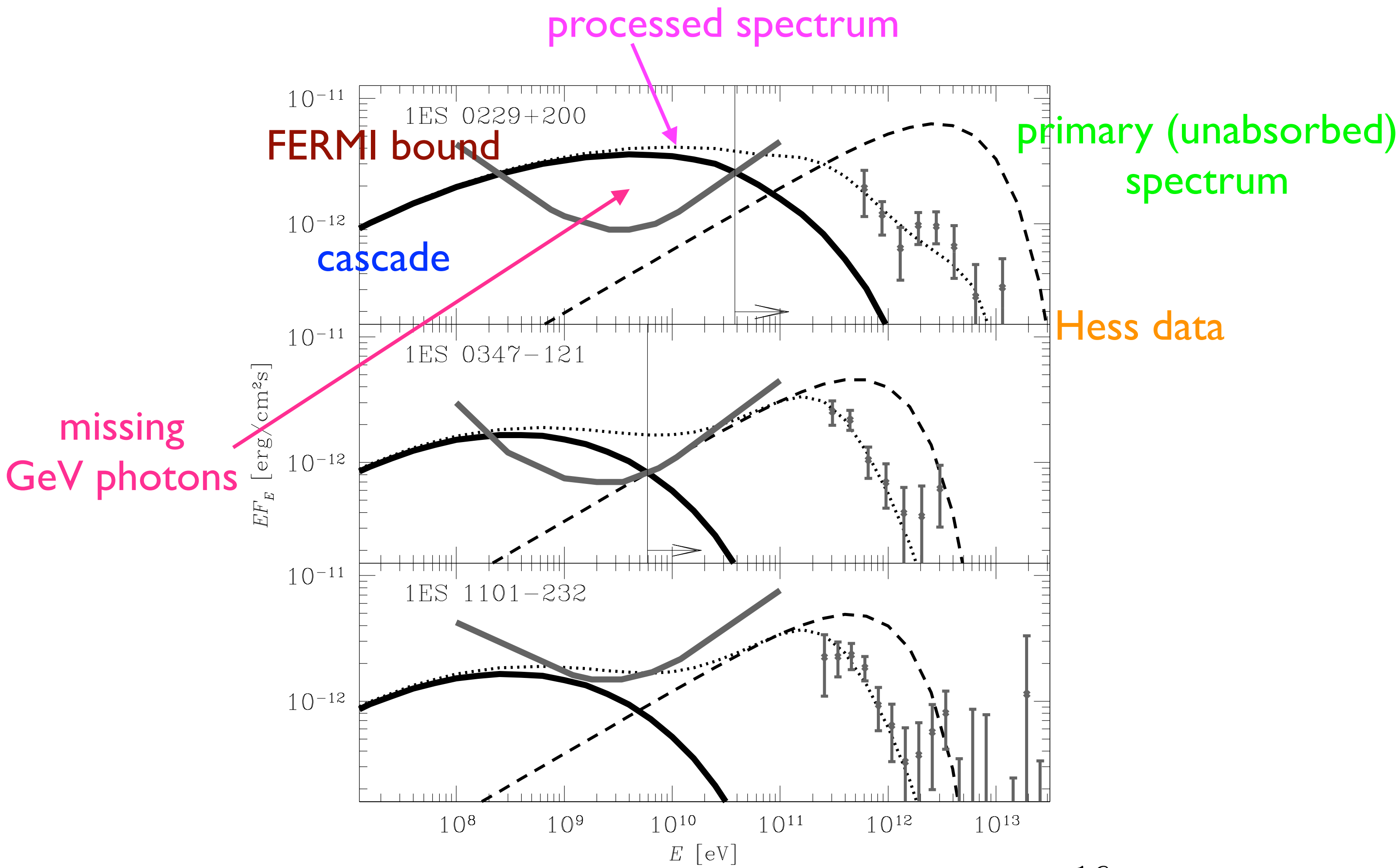

Missing GeV photons attributed to $B > 10^{-16}$ Gauss.

Uses spectral information alone.

Plasma instabilities? Broderick, Chang & Pfrommer, 2012

Stacked Analyses

Ando & Kusenko, 2010; Chen, Buckley & Ferrer, 2015.

Hints for cascade photons from (stacked) sources.

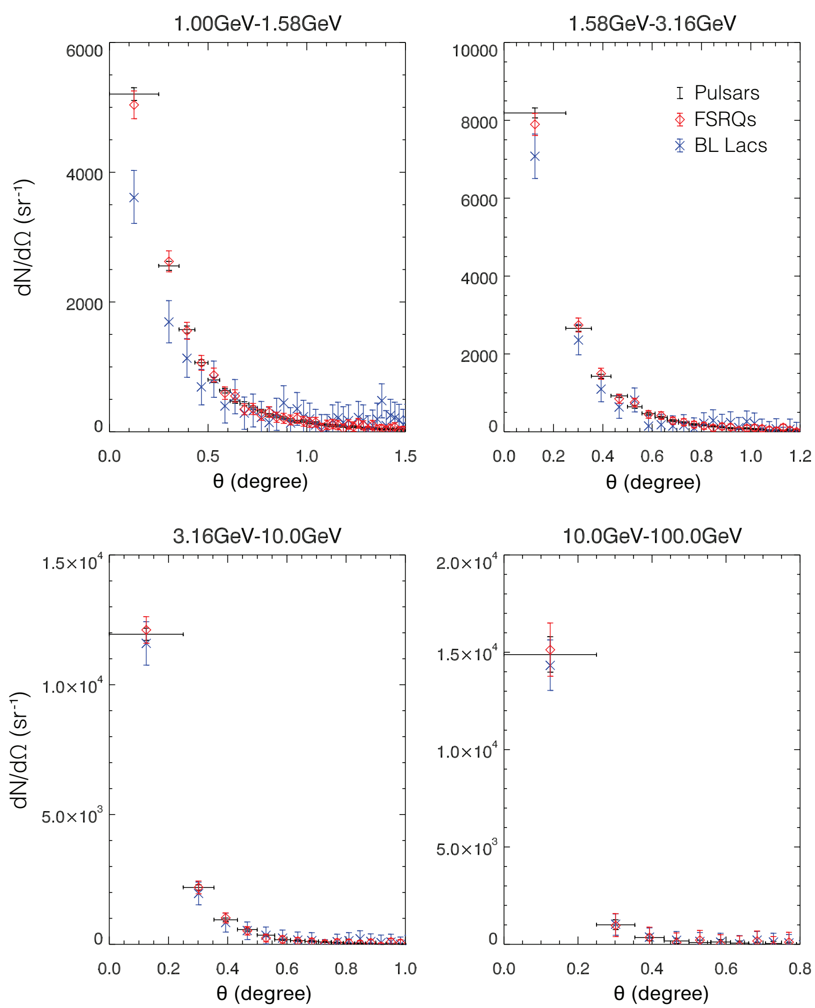

Halo Morphology: Simulations

Elyiv, Neronov & Semikoz, 2009
A. Long & TV, 2015

Non-helical B. Single mode.

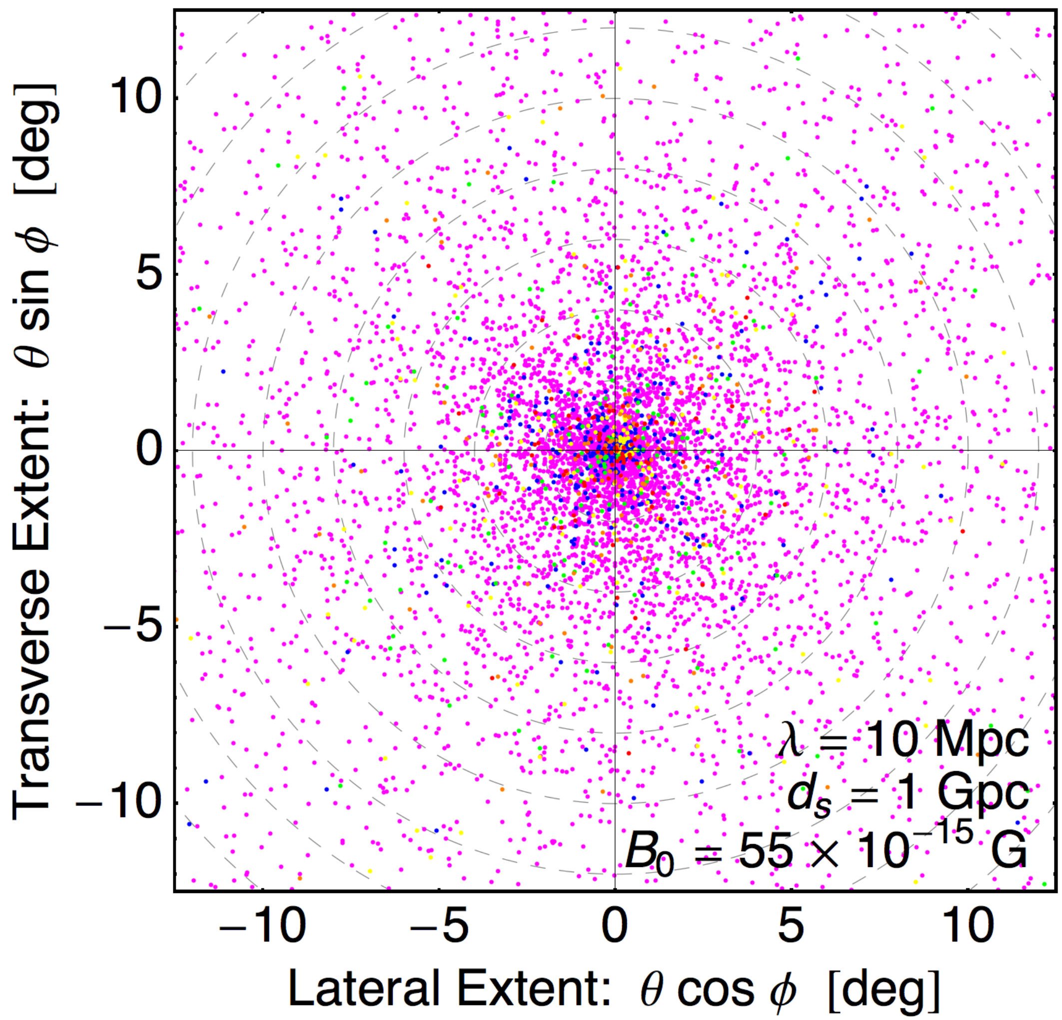

Halo Morphology: Simulations

A. Long & TV, 2015

Helical B. Single mode.

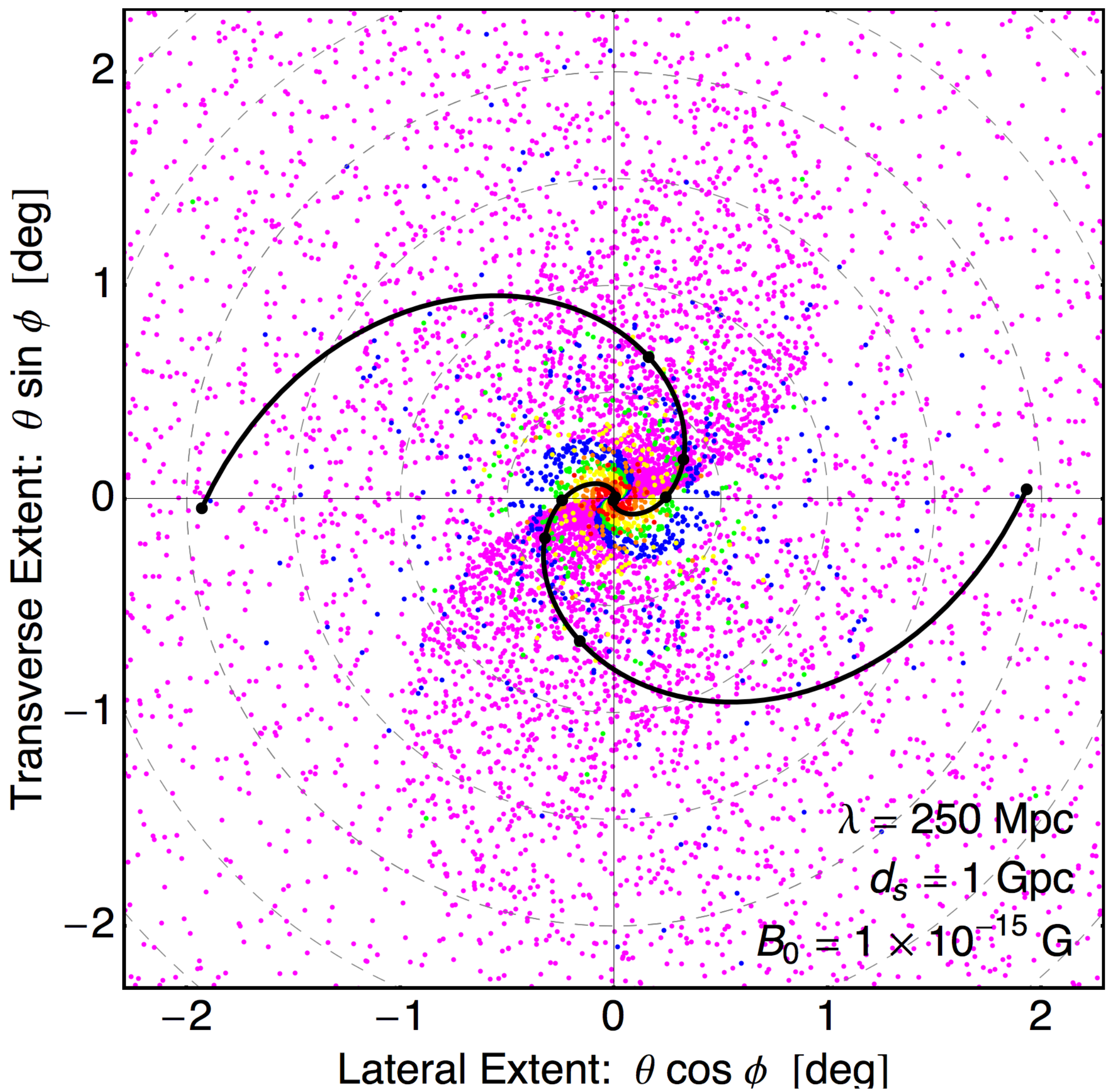

Monte Carlo Simulations

h<0

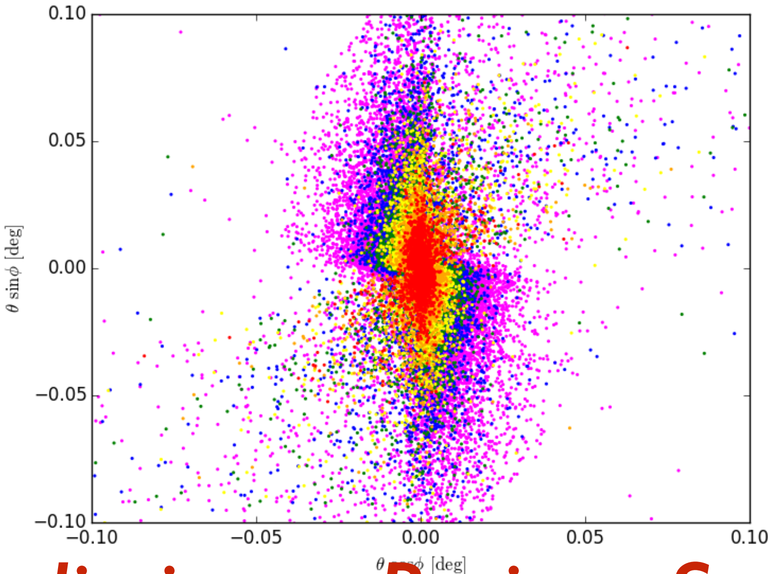

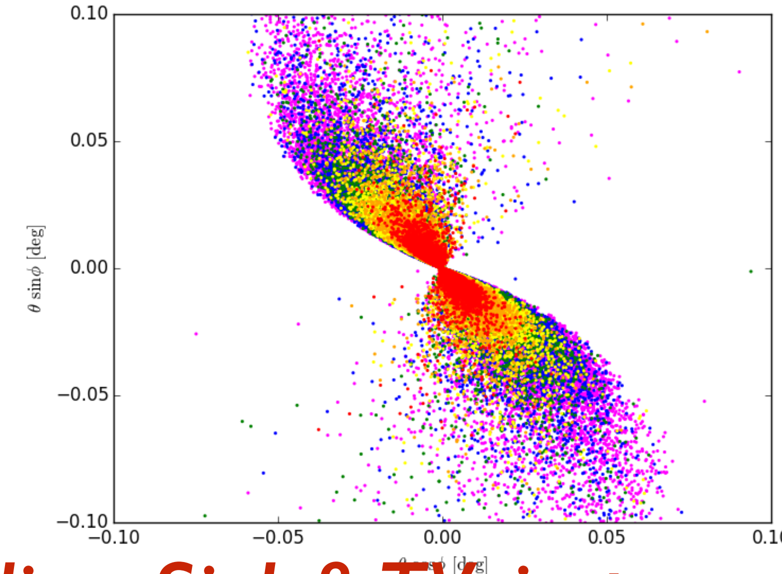

Preliminary: Batista, Saveliev, Sigl & TV, in progress

h>0

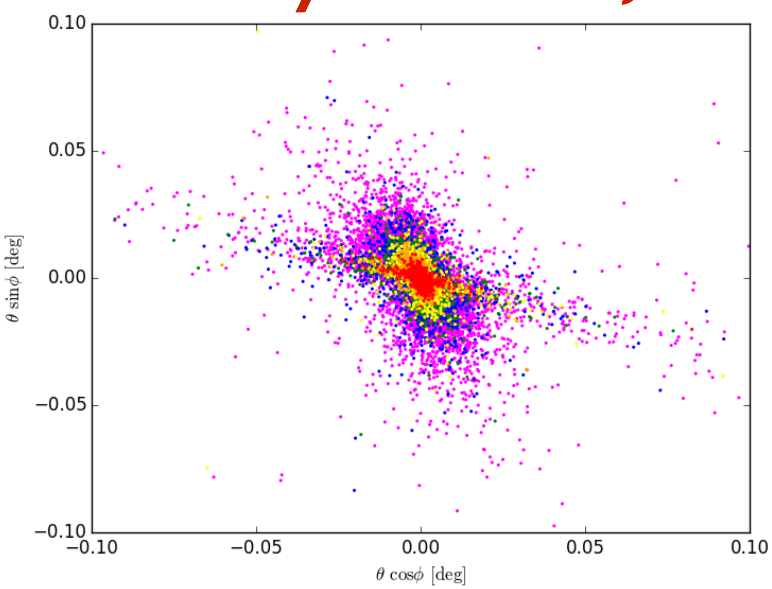

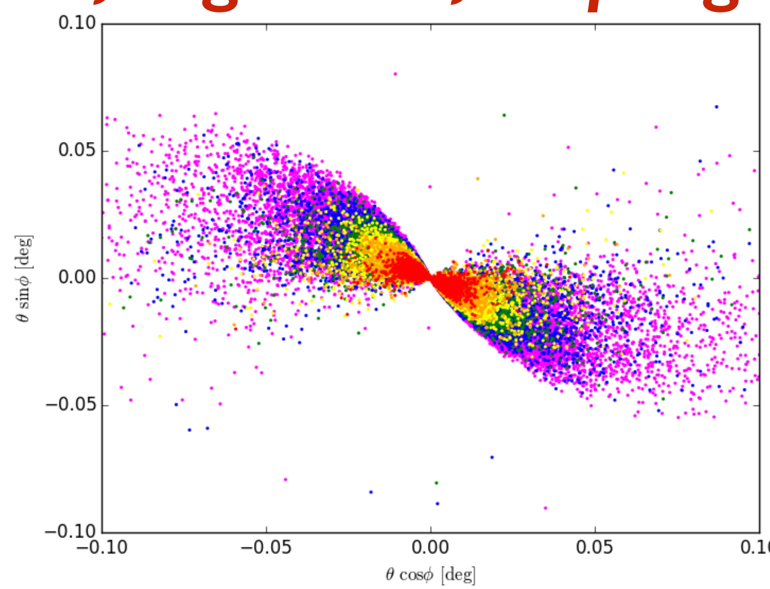

L=34Mpc

L=225Mpc

B=10E-15 G

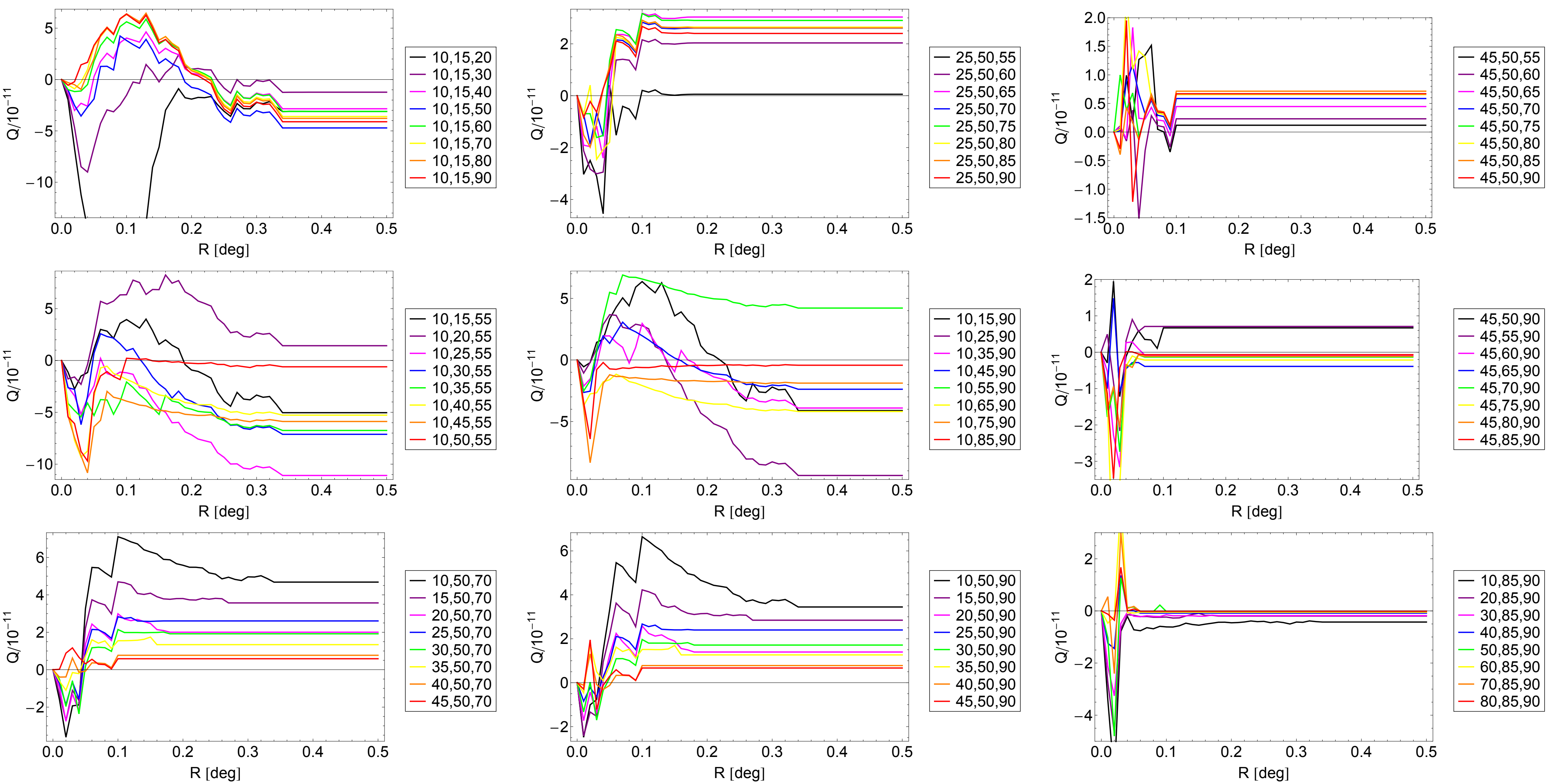

Preliminary: Batista, Saveliev, Sigl & TV, in progress

Cascade halos from (unseen*) blazars.

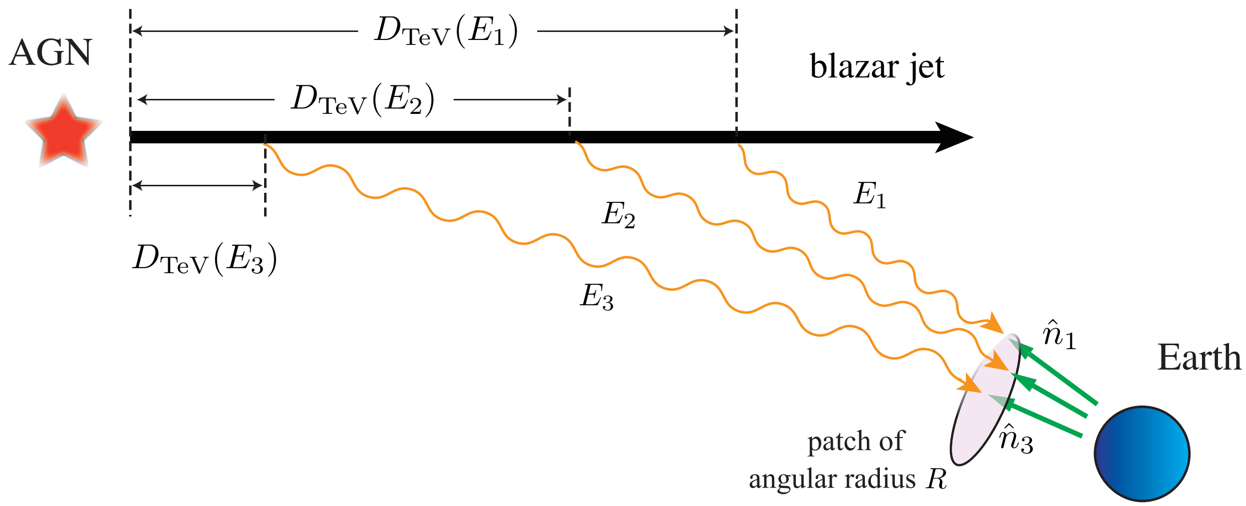

$$Q(R) = \langle \mathbf{n}_1 \times \mathbf{n}_2 \cdot \mathbf{n}_3 \rangle_R$$

**Hundreds of unseen blazars for every seen blazar.*

Gamma ray correlators

Tashiro & TV, 2013
Kahniashvili & TV, 2006

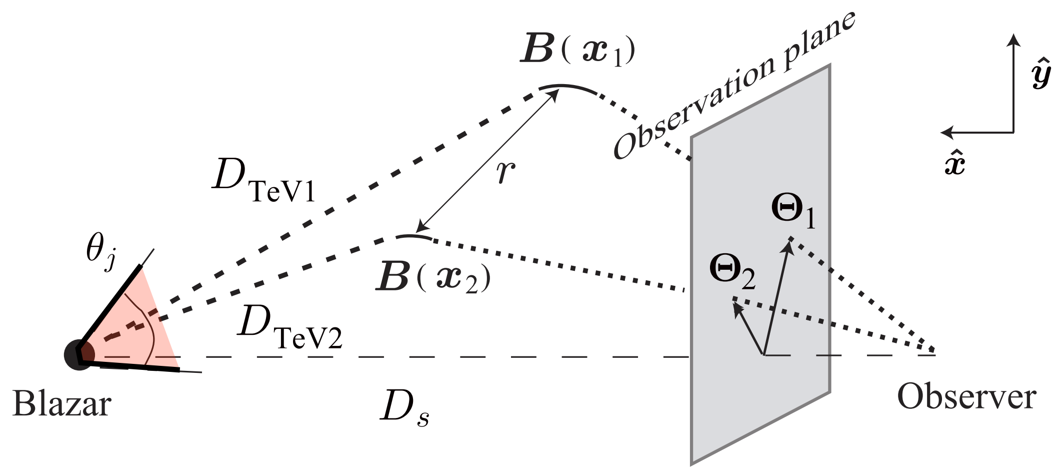

Relate correlators of arriving gamma rays to magnetic field correlators:

$$G(E_1, E_2) = \langle \boldsymbol{\Theta}(E_1) \times \boldsymbol{\Theta}(E_2) \cdot \hat{\mathbf{x}} \rangle \propto \frac{1}{2} M_H(|r_{12}|) r_{12}$$

$$\langle B_i(\mathbf{x}+\mathbf{r}) B_j(\mathbf{x}) \rangle = M_N(r) \left[\delta_{ij} - \frac{r_i r_j}{r^2} \right] + M_L(r) \frac{r_i r_j}{r^2} + M_H(r) \epsilon_{ijl} r^l$$

Different energy combinations probe magnetic field on different length scales.

Scheme

Tashiro, Chen, Ferrer & Vachaspati, 2014

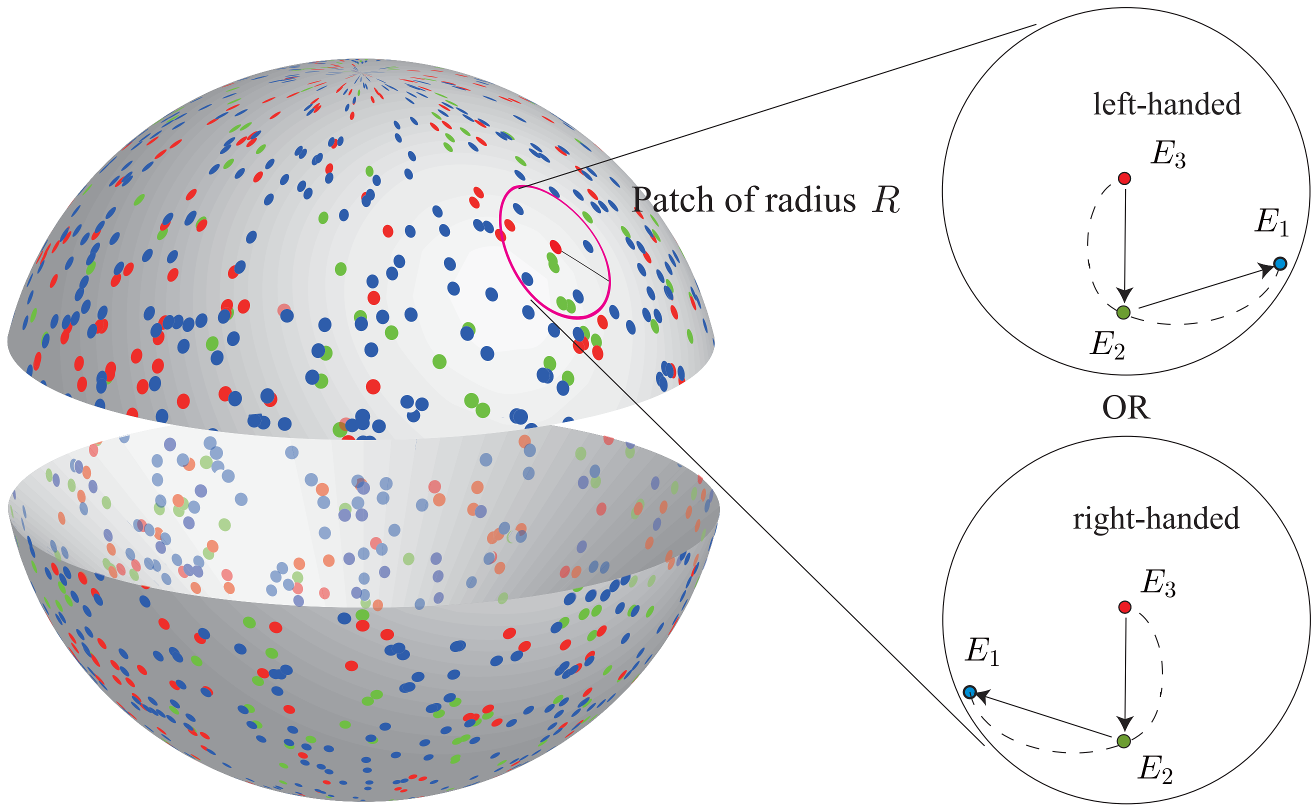

$$Q(R) = \langle \mathbf{n}_1 \times \mathbf{n}_2 \cdot \mathbf{n}_3 \rangle_R$$

Patches on the galactic sky

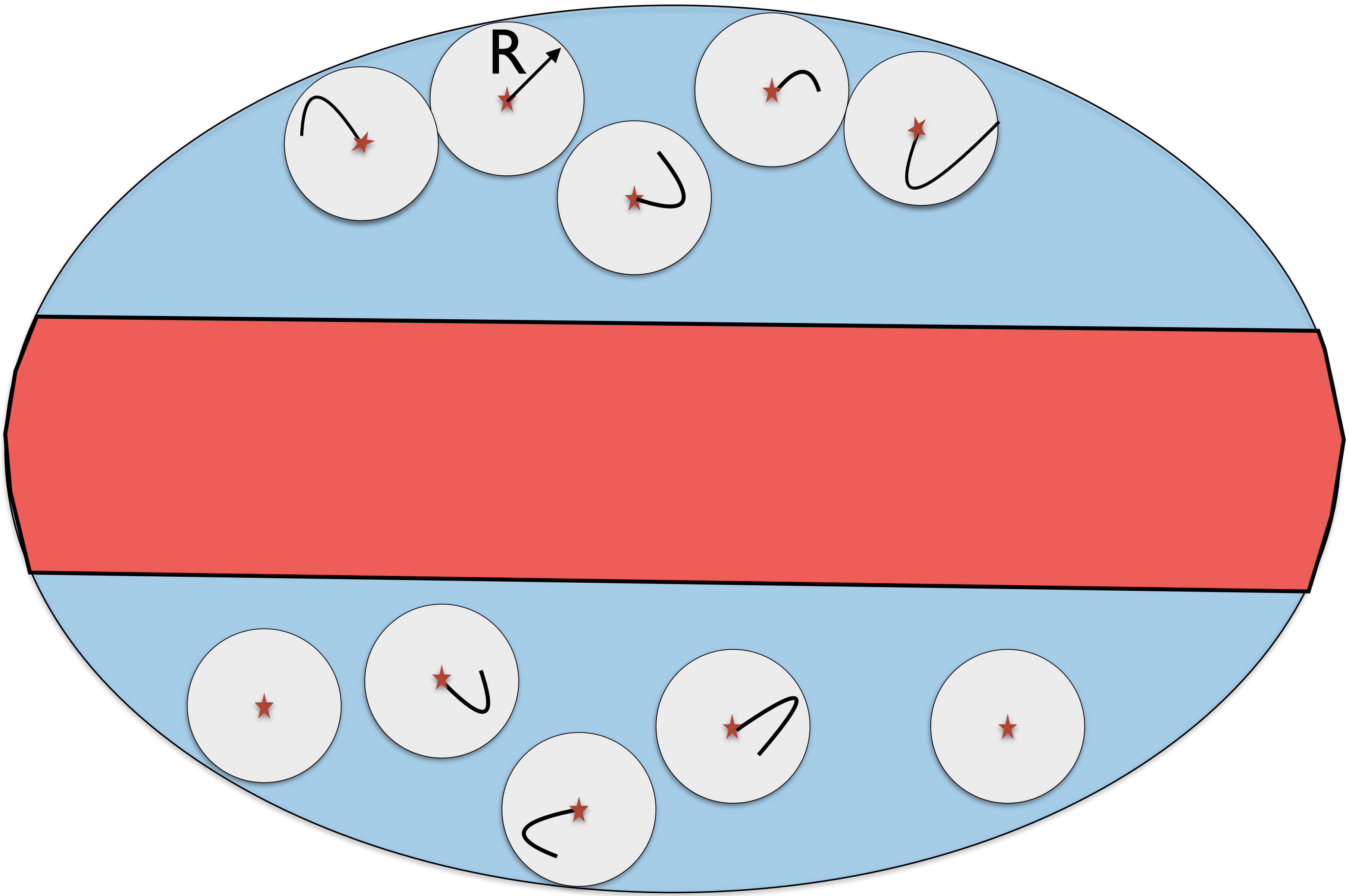

— Implement —

Find $\mathrm{Q(R)} = \langle \mathbf{n}_1 \times \mathbf{n}_2 \cdot \mathbf{n}_3 \rangle_{\mathrm{R}}$ using existing data.

Fermi-LAT CLEAN data

(through mid-September 2013)

	10-20 GeV	20-30 GeV	30-40 GeV	40-50 GeV	50-60 GeV
North($> 60°$)	3098	772	345	168	73
South($> 60°$)	2816	661	281	126	74
Total ($> 60°$)	5914	1433	626	294	147
North($> 70°$)	1322	340	156	79	40
South($> 70°$)	1146	276	120	57	30
Total ($> 70°$)	2468	616	276	136	70
North($> 80°$)	276	74	31	19	9
South($> 80°$)	293	59	20	14	12
Total ($> 80°$)	569	133	51	33	21

TABLE I. Number of photons for each energy bin.

Don't know which photons are "cascade" (signal) and which are "non-cascade" (noise).

Fermi-LAT Exposure

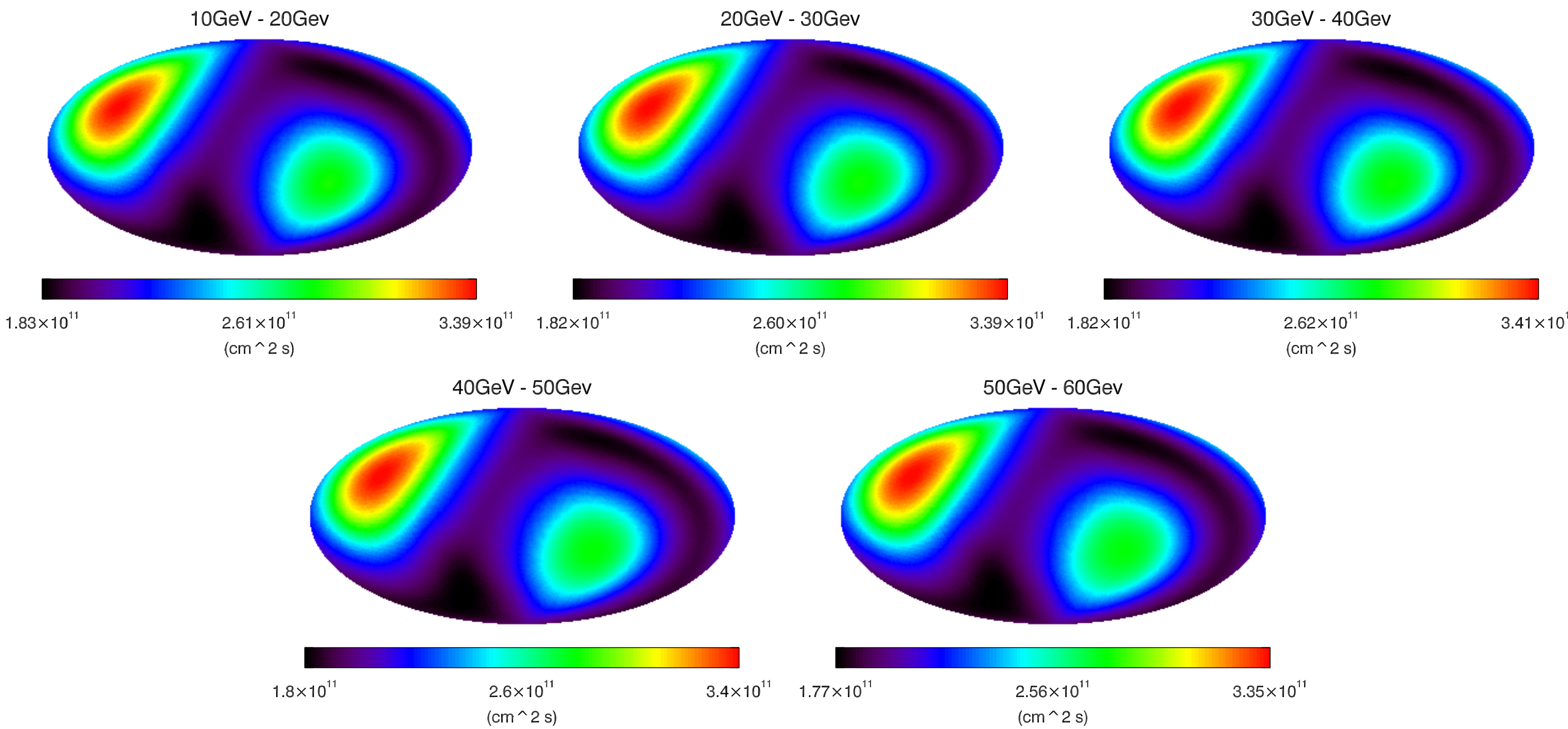

Model Q(R): features

Peak in Q(R): *Q(R)* goes to zero at small R because of patch size, and at large R because of contamination by background.

Location of peak: depends mainly on E2.

$$R_{\mathrm{peak}}(E_2) \approx R_{\mathrm{peak},0} \left(\frac{E_2^{(0)}}{E_2} \right)^{3/2}$$

based on model: Tashiro&TV

Height of peak: depends on magnetic correlation function M_H. Use height to reconstruct M_H.

Sign of peak: all peaks should have the same sign as B handedness (assumes small bending).

Fermi-LAT Pass 7 & MC with Exposure

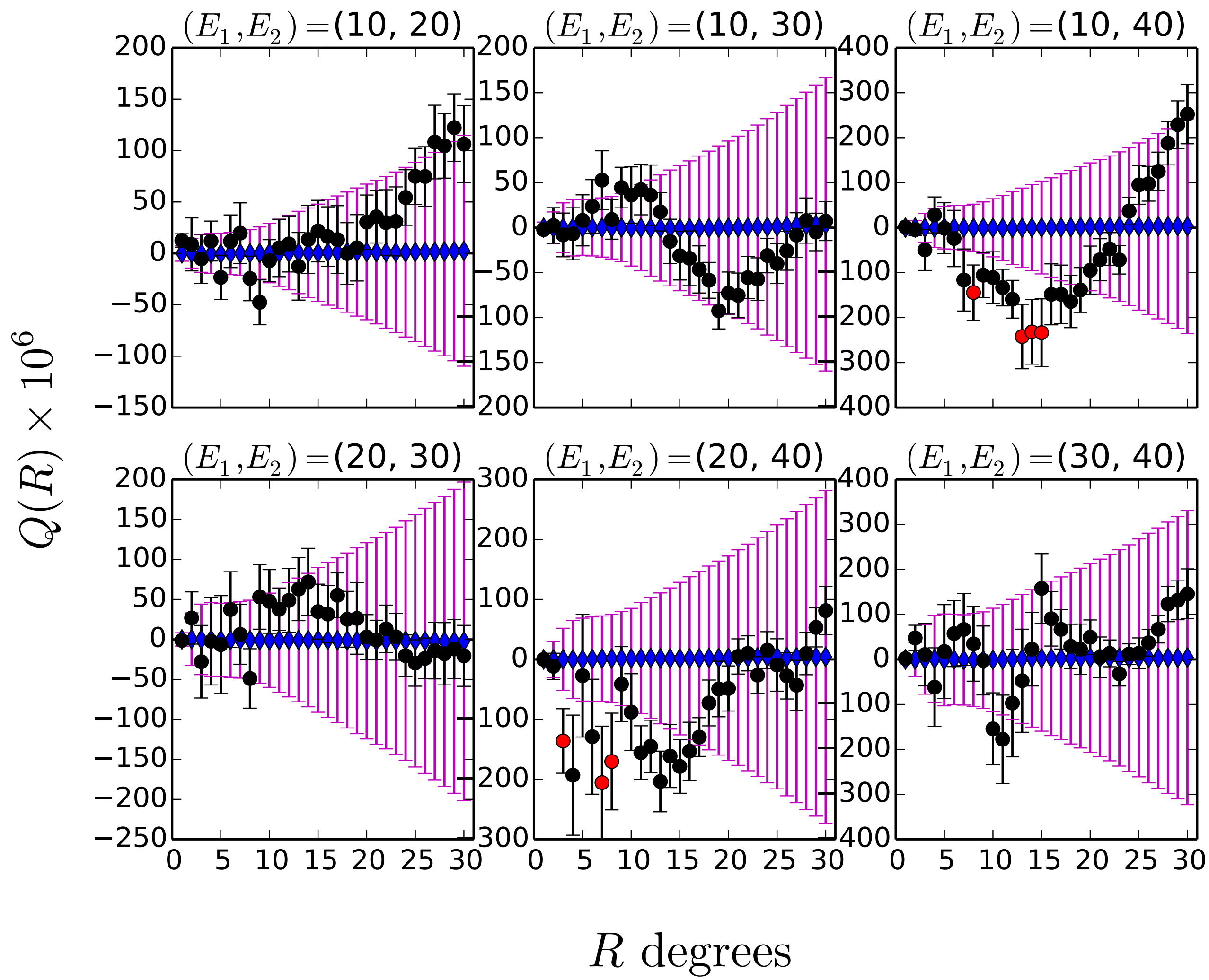

Statistical significance p~1-3% depending on the exact test.

Milky Way Contamination?

- At R less than ~20 degrees Milky Way contamination is minimal (see plots). The 30, 40 GeV data sets are especially clean.
- The signal has a peak structure whereas expect Milky Way contamination to lead to a monotonically increasing signal until very large R (~80 degrees).

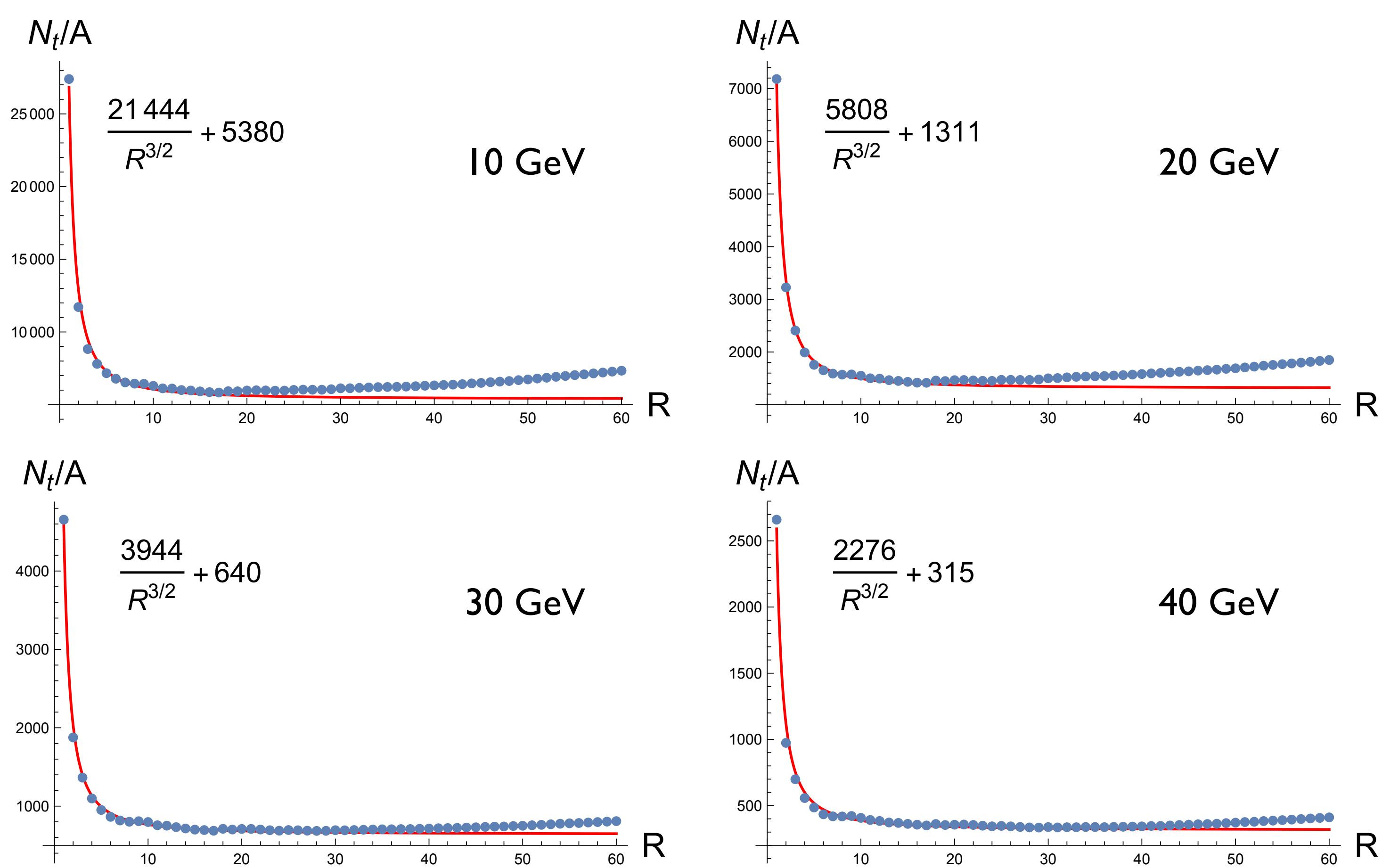

N_t/A
$\frac{21444}{R^{3/2}} + 5380$
10 GeV
25 000
20 000
15 000
10 000
10
20
30
40
50
60
R
N_t/A
$\frac{5808}{R^{3/2}} + 1311$
20 GeV
7000
6000
5000
4000
3000
2000
R
N_t/A
$\frac{3944}{R^{3/2}} + 640$
30 GeV
4000
3000
2000
1000
R
N_t/A
$\frac{2276}{R^{3/2}} + 315$
40 GeV
2500
2000
1500
1000
500
R

Fermi-LAT Pass 8 data

Significant revision of old data set plus some new data.

P7-Ultraclean vs. P8-Ultracleanveto, $b > 80°$, 50 GeV $< E <$ 60 GeV.

Event ID	**Δb**	**Δl**	**ΔE** [GeV]	Added/Dropped
5503488	-0.04	0.30	-2.7	–
4890690	0.01	-0.19	-3.1	–
4153460	-0.26	-4.64	4.5	–
15968068	0.04	-0.77	-3.6	–
8820606	-0.05	-0.19	1.0	–
2970731	0.02	-0.50	-3.0	–
4550395	0.01	0.08	-0.5	–
6030395	0.03	0.43	-0.8	–
416328	0.01	1.0	-0.4	–
3628595	0.03	-0.01	2.2	–
4897015	0.08	0.74	-0.2	–
3518924	-0.11	0.58	0.1	–
6336309	-0.07	0.11	1.7	–
3193818	-0.01	0.57	-0.5	–
4677466	0.01	-0.95	-1.3	–
7533363	3.8	0.04	2.8	–
4715735	0.01	-0.03	-0.7	–
6586539	0.01	0.004	-6.6	–
5554658	0.01	0.05	-0.1	–
5082626	0.08	0.12	-1.0	Source in P8
7693919	0.58	-2.25	-2.4	Source in P8
4873062	0.06	0.57	1.8	Source in P8
11159439	0.01	-0.02	-1.8	Source in P8
7316118	–	–	–	Not in P8
4708017	–	–	–	Not in P8
672765	–	–	–	Not in P8
5706981	–	–	–	Not in P8
6745444	–	–	–	Not in P8
5092183	–	–	–	Not in P8
5971682	–	–	–	Not in P8
5475541	–	–	–	Not in P8
4794054	–	–	–	Not in P8

In addition the following new events are new in P8: 1391689, 1851782, 2056790, 2077838, 2126241, 2347872, 2580764, 3045655, 3605689, 3781886, 4086287, 5387126, 5431401, 5627146, 5803756, 5988863, 6122538, 7030348, 7418123, 8332252, 10163628, 10602321, 10828931, 11008279.

Pass7 vs. Pass8

Wenlei Chen

Pass7 ULTRACLEAN week 9 – week 328
10 GeV – 20 GeV |GLAT|>50°

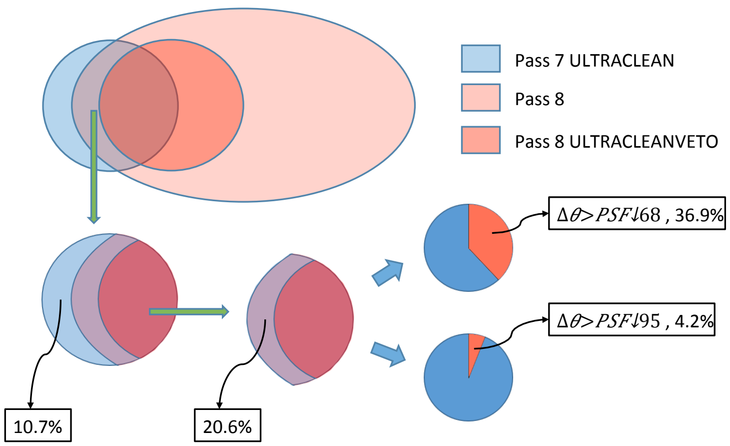

Pass7 ULTRACLEAN week 9 – week 328
20 GeV – 30 GeV |GLAT|>50°

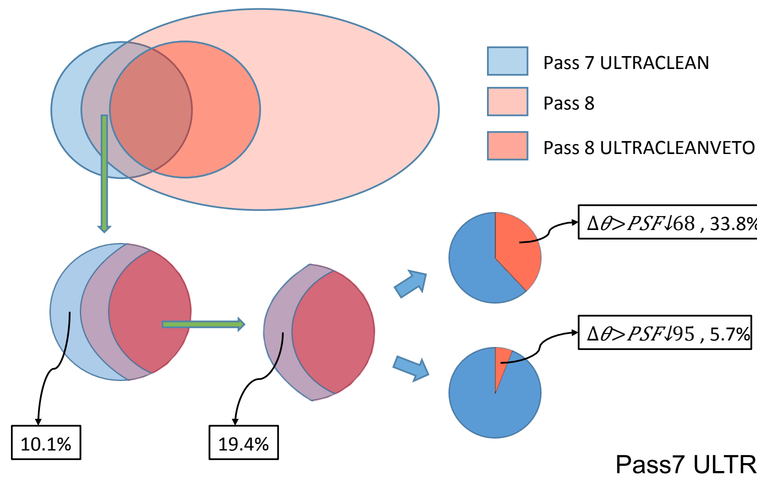

Pass7 ULTRACLEAN week 9 – week 328
30 GeV – 40 GeV |GLAT|>50°

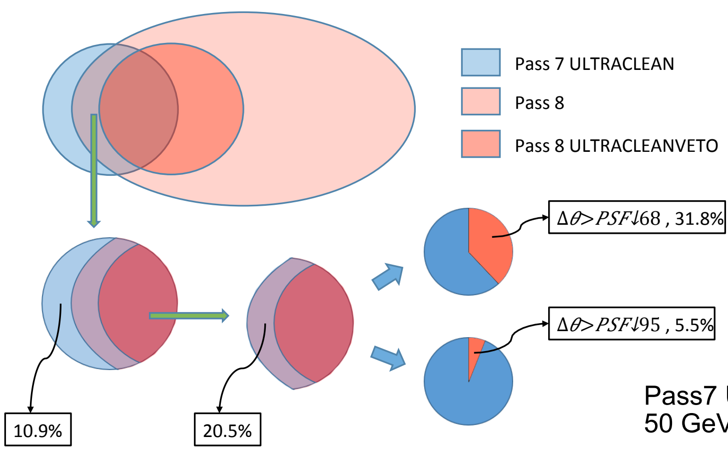

Pass7 ULTRACLEAN week 9 – week 328
40 GeV – 50 GeV |GLAT|>50°

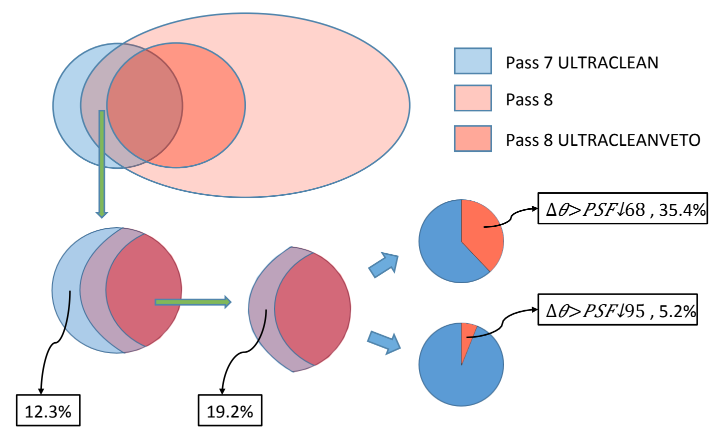

Pass7 ULTRACLEAN week 9 – week 328
50 GeV – 60 GeV |GLAT|>80°

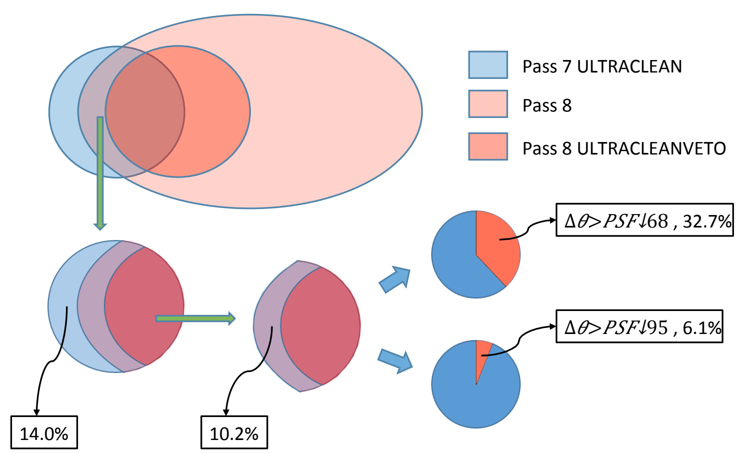

Fermi-LAT Pass 7 & MC with Exposure

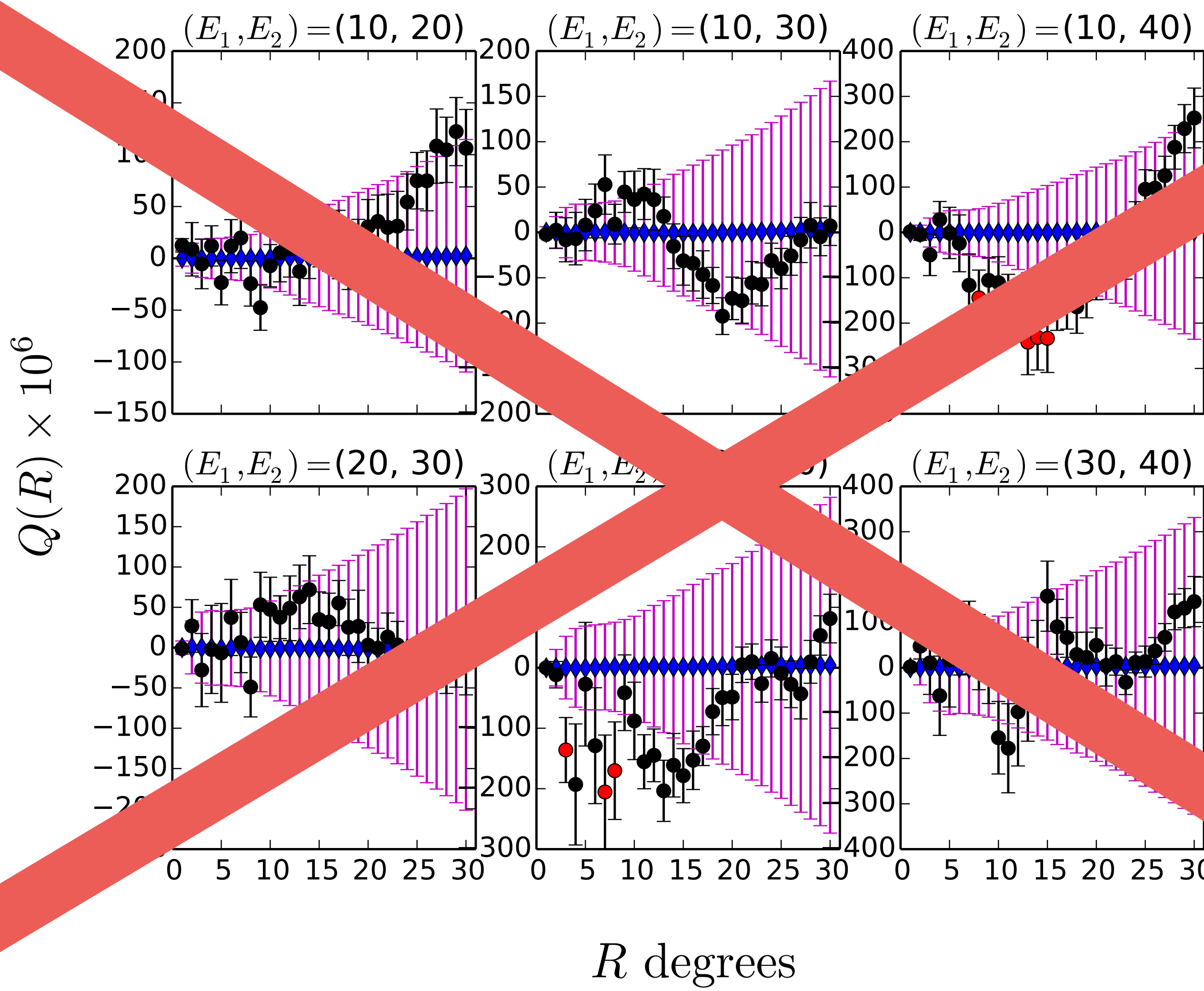

Statistical significance p~1-3% depending on the exact test.

Fermi-LAT Pass 8 & MC with Exposure

Preliminary: Chen, Ferrer, Tashiro & TV, in progress

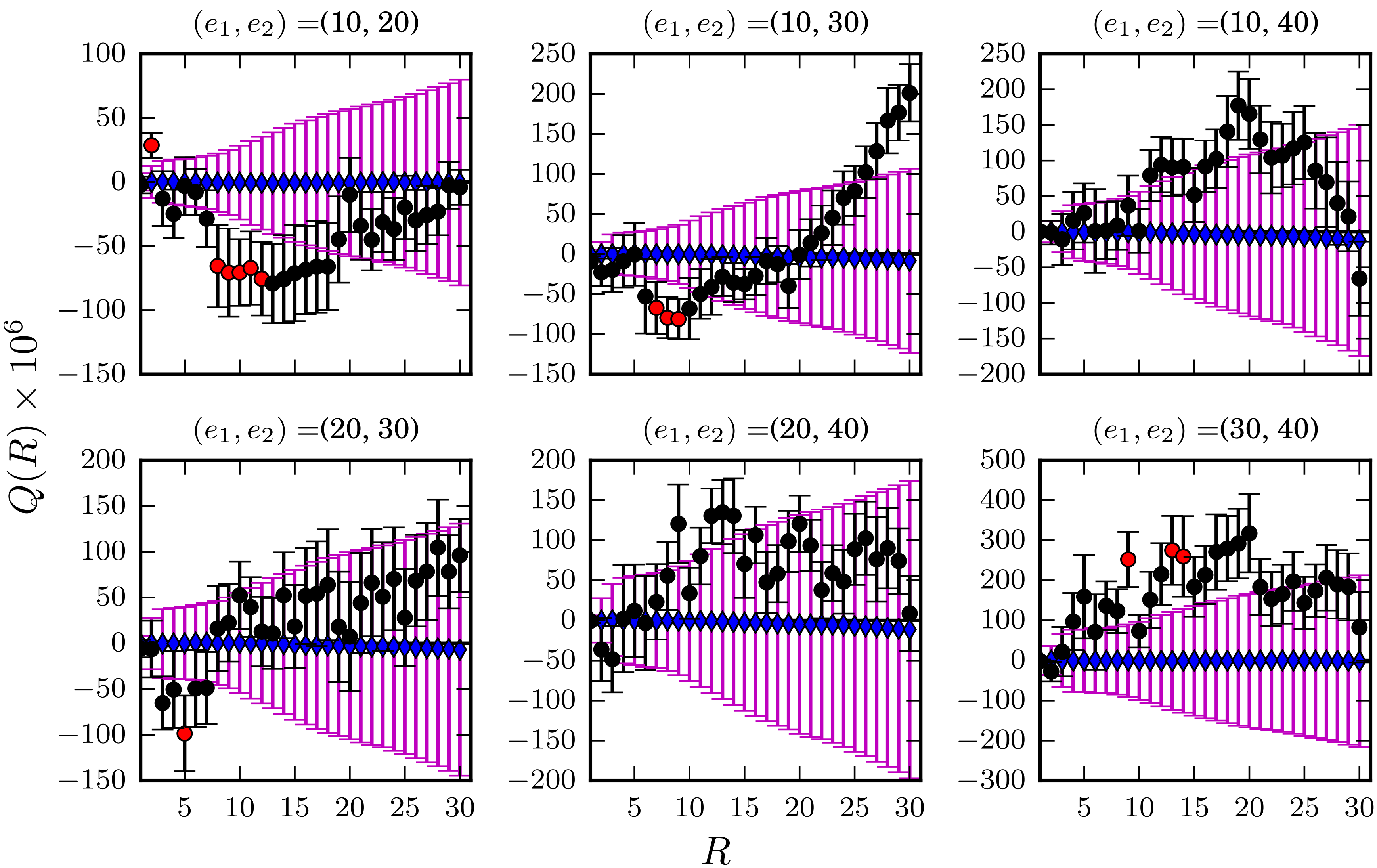

Up to week 328 (as in Pass7) but in Pass 8.

North/South, week 328, Pass 8

Preliminary: Chen, Ferrer, Tashiro & TV, in progress

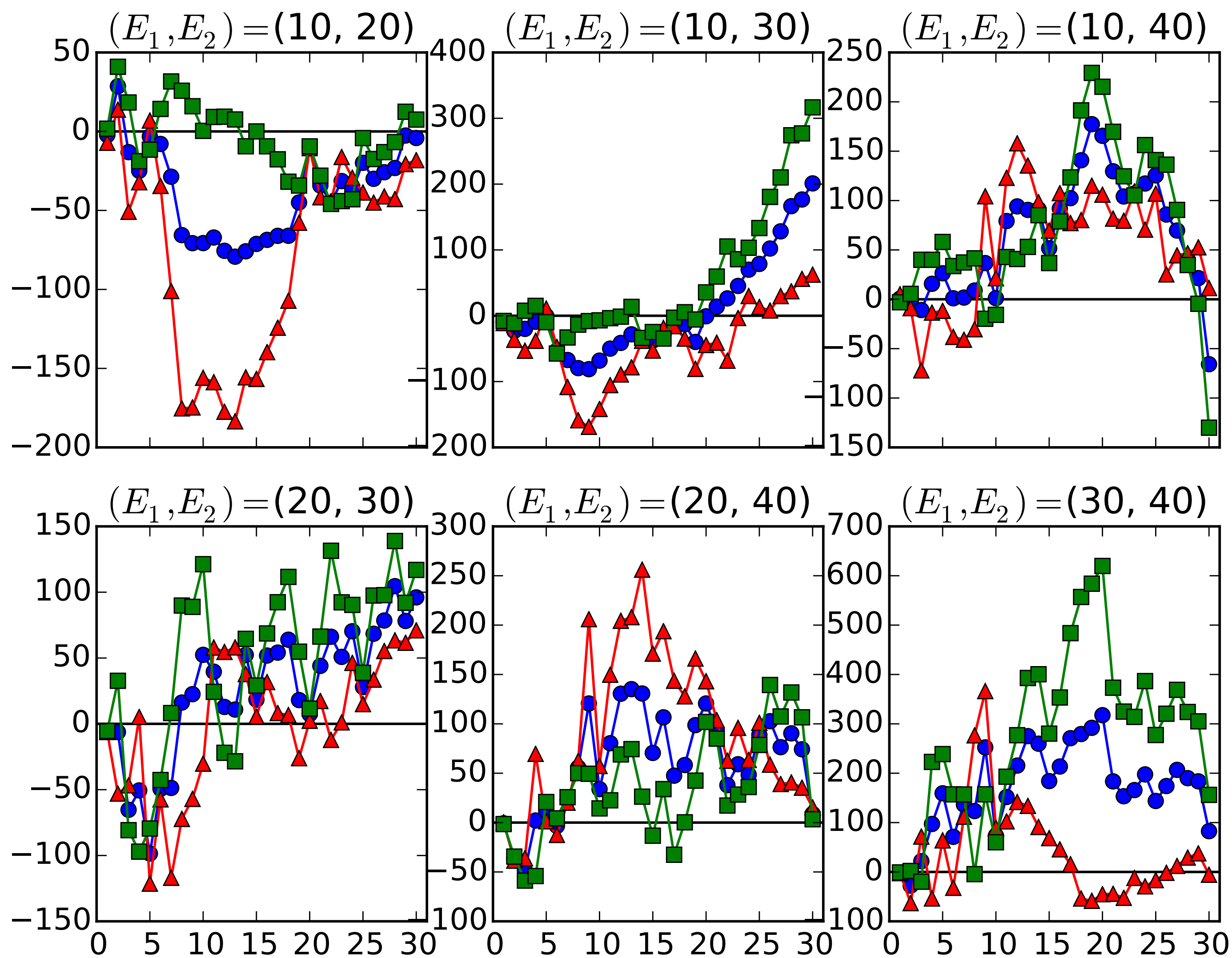

Week 369, Pass 8

Preliminary: Chen, Ferrer, Tashiro & TV, in progress

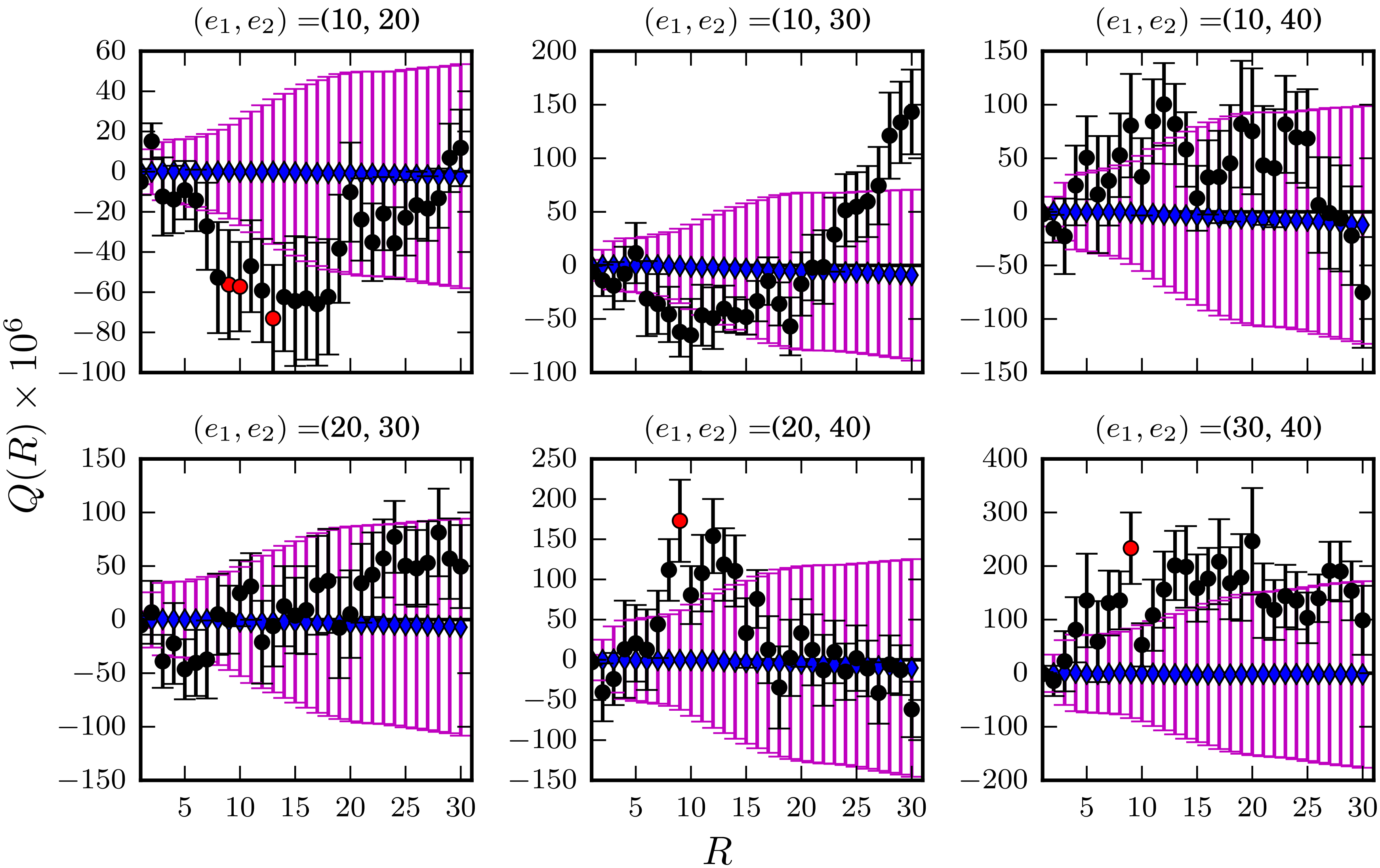

North/South, Week 369, Pass 8

Preliminary: Chen, Ferrer, Tashiro & TV, in progress

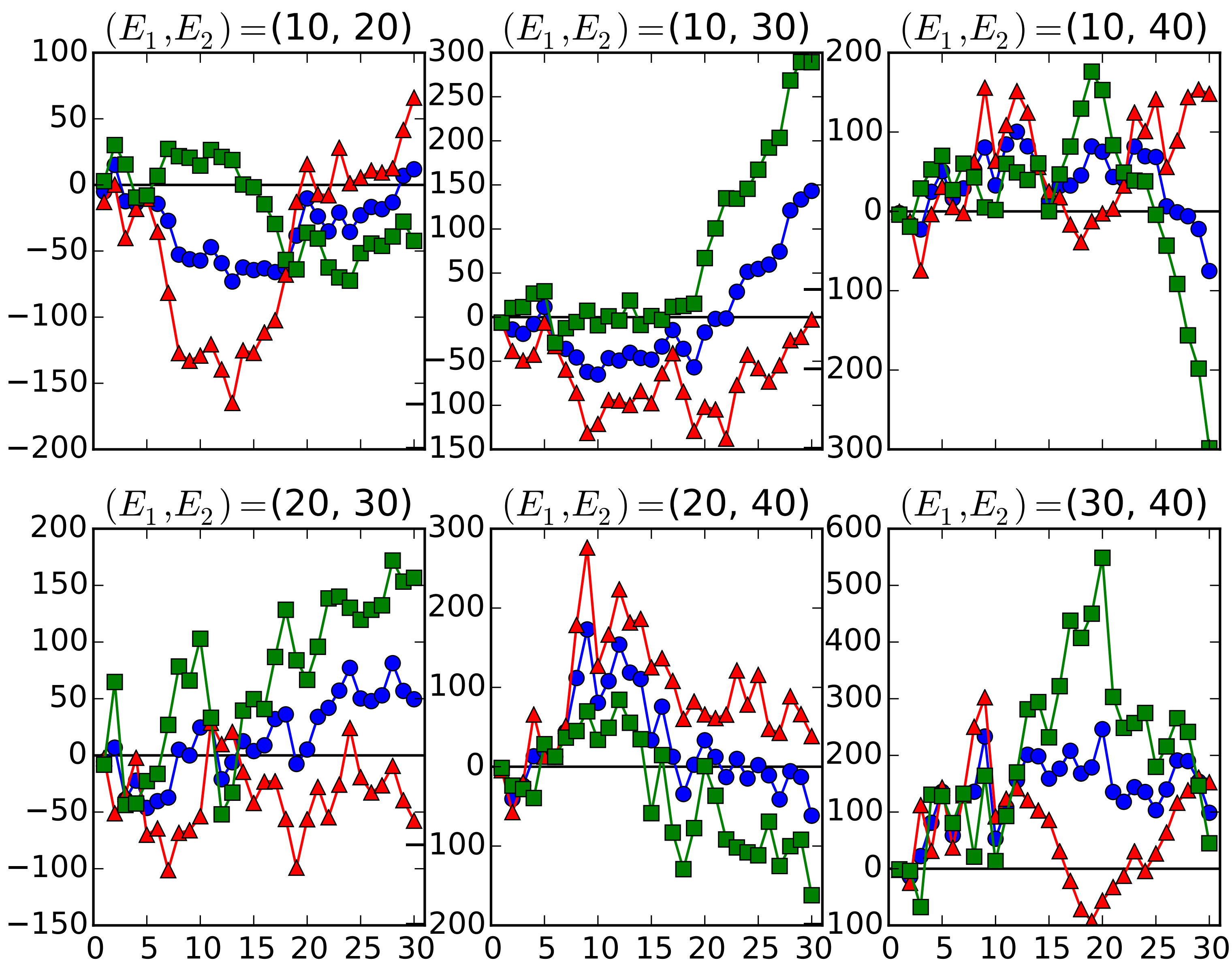

Conclusions

Virtues of helicity:

- Magnetic helicity *aids* detection of B and allows us to measure the magnetic power spectra.
- Helicity can distinguish cosmological/astrophysical fields, primordial/causal mechanisms, baryo/lepto-genesis.

Effect of helicity:

- Analysis+simulations show spirals in cascade gamma rays.

Observation of helicity:

- Analysis of Pass8 data hints at a signal but not conclusive (yet).